Enhanced Diffusion due to Active Swimmers at a Solid Surface

Gastón Miño,[1] Thomas E. Mallouk,[2] Thierry Darnige,[1] Mauricio Hoyos,[1] Jeremi Dauchet,[1] Jocelyn Dunstan,[3] Rodrigo Soto,[3] Yang Wang,[2] Annie Rousselet,[1] and Eric Clement[1]

[1]*PMMH, ESPCI, CNRS (UMR 7636) and Université Paris 6 and Paris 7, 10 rue Vauquelin, 75005 Paris, France*
[2]*Department of Chemistry, The Pennsylvania State University, University Park, Pennsylvania, USA*
[3]*Departmento de Física, FCFM, Universidad de Chile, Santiago, Chile*

(Received 1 September 2010; published 25 January 2011)

We consider two systems of active swimmers moving close to a solid surface, one being a living population of wild-type *E. coli* and the other being an assembly of self-propelled Au-Pt rods. In both situations, we have identified two different types of motion at the surface and evaluated the fraction of the population that displayed ballistic trajectories (active swimmers) with respect to those showing random-like behavior. We studied the effect of this complex swimming activity on the diffusivity of passive tracers also present at the surface. We found that the tracer diffusivity is enhanced with respect to standard Brownian motion and increases linearly with the activity of the fluid, defined as the product of the fraction of active swimmers and their mean velocity. This result can be understood in terms of series of elementary encounters between the active swimmers and the tracers.

DOI: 10.1103/PhysRevLett.106.048102 PACS numbers: 87.17.Jj, 05.40.−a, 47.63.Gd, 47.63.mf

Since the pioneering work of Wu and Libchaber [1], considerable efforts have been made to understand hydrodynamic properties of active suspensions. Generally speaking, this is the name borne by fluids laden with self-swimming entities such as bacteria [2–5], algae [6,7], or collections of active artificial swimmers [8]. Assemblies of microscopic motors dispersed in a fluid display emergent properties that differ strongly from passive suspensions. The momentum and energy transfer balances as well the constitutive transport properties are deeply modified by the momentum sources distributed in the bulk [2,9]. Some of these anomalous properties have already been identified, such as active diffusivity [1,2], anomalous viscous response [7,10], active transport, and mixing [11], as well as the possibility to use fluctuations to extract work [12]. The presence of living and apparently gregarious entities also offers the possibility to move collectively and organize at the mesoscopic or macroscopic level in the form of flocks and herds [9,13]. Similar collective effects were also identified in suspensions of self-propelled inorganic particles [14]. In the bulk, swimming bacteria with flagella such as *E. coli* create in the far field limit a force-dipole velocity field, and, consequently, experience a hydrodynamic attraction toward surfaces [15]. Then, it has been observed that *E. coli* smooth out their run-and-tumble movement and spend long times parallel to the surface undergoing circular motion as a consequence of the torque-free condition [16,17]. When the concentration becomes large, the *E. coli* population eventually associates collectively to form a biofilm. Even in the low concentration limit, the quantitative analysis of the near surface motion increases tremendously in complexity, a reason being the close field hydrodynamic forces that become prevalent and require a complex treatment of the lubrication hydrodynamic fields. However, even in this frame of description, it remains unclear whether the motion close to the surface is hydrodynamically stable and if the presence of thermal noise is essential to account for the bacterium dwelling time at a surface [18]. Beyond the hydrodynamic interactions, more complex ingredients may come into play, such as surface interaction potentials (electrostatic or van der Waals) [19] or more refined details of the bacterium physiology such as swimming speed variations and desynchronization during bacteria cell cycle [20,21]. From the perspective of providing a fully consistent treatment of active hydrodynamics, with important applications for understanding bacterial transfer in biological microvessels, microfluidic devices, or the formation of biofilms, a reliable description of fluid activity in the vicinity of a solid surface is strongly needed. In this Letter, to tackle this open and timely question, we compared the behavior of two kinds of active micrometric swimmers: wild-type *E. coli* K-12 and artificial self-propelling rods [8], with completely different propulsion mechanisms. In both cases, we monitor the swimmers' motions and their ability to activate, beyond Brownian motion, passive tracers, hence characterizing the active momentum transfer to the fluid.

Following the experimental procedure described in Ref. [15], wild-type *E. coli* K-12 were grown overnight in rich medium (Luria broth). After washing, they were transferred into MMAP, a motility medium supplemented with K-acetate (0.34 m*M*) and polyvinyl pyrolidone (PVP, 0.005%). They were incubated for at least an hour in that medium and, in some cases, so-called ''baby cells'' were selected by centrifugation and resuspended in MMAP. To avoid bacterial sedimentation (isodense conditions), Percoll was mixed with MMAP (1 vol/1 vol). We checked

that under these conditions, the suspending fluid was still Newtonian (viscosity $\eta = 1.28 \times 10^{-3}$ Pa s at 22 °C). The overall concentration of bacteria was controlled such as to prepare suspensions between 10^9 and 10^{10} bacteria/ml. To study the effect of bacterial activity on the diffusivity of passive tracers, latex beads of 1 or 2 μm diameter (Beckman-Coulter, density $\rho = 1.027$ g/ml) were added to the suspensions. Experiments were performed in 110 μm thick chambers, built with two horizontal microscope cover slips separated by a glass spacer. To avoid sticking, cover slips were coated with PVP. The biological sample consisted in a drop of liquid (20 μl) placed between the two slides. The suspension was observed under an inverted microscope (Zeiss-Observer, Z1-magnification 40 ×) connected to a digital camera. The observation field ΔV was 96×128 μm^2 and 5 μm in depth. In a first series of experiments, we measured the bacterial density profile through the entire height of the chamber. We obtained profiles similar to the ones published by Berke and coworkers [15], namely, a flat density in the bulk and a strong density increase near the surfaces. However, the wild-type *E. coli* we used was significantly less attracted by the surfaces (2.5 times increase in density within 10 μm of the surface) than a mutant *E. coli* strain that does not display tumbling motion [16,17]. Another series of experiments was performed with bimetallic Au-Pt self-propelled rods (length 1.2 μm and diameter 0.4 μm) that are very similar in size to the *E. coli* cell body (1–2 μm long, 0.8 μm diameter) but have no flagella (15 μm long for *E. coli*) [see insets in Figs. 1(c) and 1(f)]. They also have a much higher density ($\rho = 17$ g/ml). In the presence of 1%–10% hydrogen peroxide, these particles are propelled in the axial direction towards the platinum end by the catalytic decomposition of the peroxide fuel [8]. Recent experiments and simulations are consistent with self-electrophoresis as the dominant propulsion mechanism [22,23]. Here, the mode of propulsion is intrinsically different from the flagellar one. The experiments were conducted in a similar fashion to those involving *E. coli*, but in an open chamber (without the upper wall), in order to allow the oxygen bubbles produced in the reaction to escape from the cell. The concentration of H_2O_2 was varied, as well as the concentration of active rods [$n = (3\text{–}20) \times 10^6$ rods/ml]. We also used passive tracers [1 μm (Dynal-MyOne, $\rho = 1.8$ g/ml) or 2 μm (Beckman-Coulter, $\rho = 1.027$ g/ml)] to follow the Au-Pt rod fluid activation. In all cases, all the particles in the suspension were localized at the bottom of the chamber due to sedimentation. Short videos (20 s duration at 20 frames/s) were used to track both bacterial and self-propelled rods motion.

In the following, we only focus on bacteria and rods moving close to the surface (less than 5 μm). In both cases, we observed that not all swimmers display similar trajectories. This was expected, as for wild-type bacteria, the run or tumble dynamics may depend strongly on the microenvironment or on the position in the cell cycle. For Au-Pt rods, this is also consistent with previous

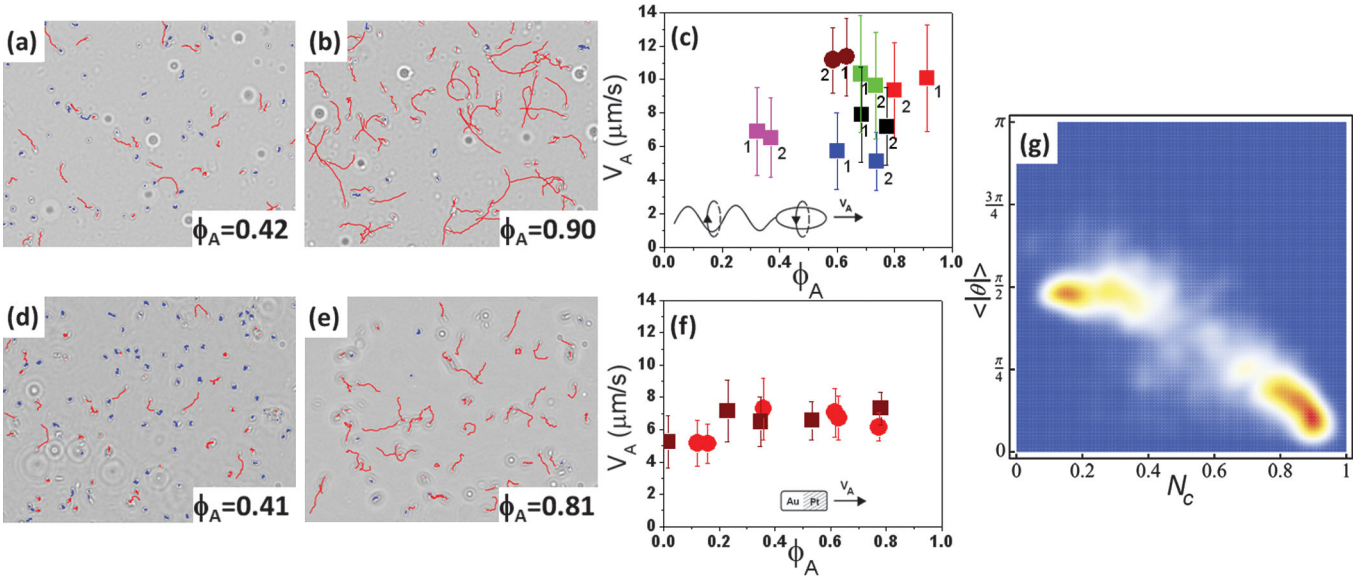

FIG. 1 (color). Identification of the swimmer populations by tracking active swimmers (red tracks) and random swimmers (blue tracks), ϕ_A is the corresponding fraction of active swimmers. Panels (a),(b),(g) correspond to *E. coli* see inset in (c)] and panels (d),(e) correspond to Au-Pt rods [see inset in (f)]. The round black circles in (a),(b) are 2 μm latex beads; the white small circles in (d),(e) are 1 μm Dynal beads. Panels (c),(f) display the relation between the active swimmer's mean velocity V_A and ϕ_A. In (c) are 6 independent experiments with *E. coli*: 1N cells (brown, red, and green), mixture of 1N and 2N cells (black), and 2N cells (pink, blue). Labels (1) and (2) are for $\langle N \rangle = 100$ and $\langle N \rangle = 200$ cells in the observation field, respectively. (f) Au-Pt rods with varying proportions of inactive Au rods (2 independent experiments). (g) density probability of the observed bacterial tracks in the $(N_c, \langle |\theta| \rangle)$ space. The color map goes from blue for vanishing probability to red for high probability. Two clusters are identified, centered at (0.9, 0.3) and (0.17, $\pi/2$), corresponding, respectively, to the active and random swimmers.

observations that, even within a single batch, electrochemically grown rods have a range of catalytic activity [8]. We developed a tracking program to analyze the short videos and obtained tracks for each swimmer present in the field. We identified two major types of motion: a ballistic and a random one [see Figs. 1(a), 1(b), 1(d), and 1(e)], and the swimmers that follow these motions are called "active" swimmers and "random" swimmers, respectively. To discriminate all the tracks systematically, two parameters were defined. The first parameter $\langle|\theta|\rangle$ is the mean angle between two successive steps. For example, $\langle|\theta|\rangle = 0$ for straight trajectories and $\langle|\theta|\rangle = \pi/2$ for a purely random walk. The second discriminating parameter is based on the minimal circle diameter L that encompasses a given trajectory of duration T. For an acquisition time δt (1/20 s) and a mean step size δr, the number $N_c = \frac{L\delta t}{T\delta r}$ is computed. When N_c is close to 1, the trajectory is associated with a straight line, whereas when N_c is small, its value points to diffusive motion. Therefore, each track is associated with these two numbers, and in the $(N_c, \langle|\theta|\rangle)$ parameter space we could identify two clusters that clearly differentiated the active and random swimmers [see Fig. 1(g)]. Nevertheless, for very small or interrupted trajectories, the separation procedure remained ambiguous, so we systematically discarded tracks shorter than 10 steps. In the case of artificial swimmers, we also managed to control *a priori* the fraction of active swimmers by adding inactive rods (made only of gold) and keeping the total number of rods at the surface constant. According to the trajectory classification, a fraction ϕ_A of active swimmers was determined. Thus, for a mean number $\langle N\rangle$ of swimmers, identified in the field of vision, we define a density of "active swimmers" as $n_A = \phi_A\langle N\rangle/\Delta V$. In Fig. 1, we display tracks during a time lag $\tau = 1.5$ s, for two populations of swimmers [1(a) and 1(b), bacteria, and 1(d) and 1(e), Au-Pt rods], having different ϕ_A [1(a) and 1(d), small active fraction, and 1(b) and 1(e), high active fraction]. In Figs. 1(c) and 1(f), we present the mean velocities of active swimmers V_A as a function of their fraction ϕ_A, for different experiments with bacteria and active rods. In the case of the bacterial suspension, we also tried several synchronization protocols to select bacteria, at different positions in the cell cycle, showing different swimming characteristics. We were able to produce "baby-bacteria" populations (1N short cells, 1.12 μm long) which were found to have a ϕ_A larger than the more mature bacteria populations (2N long cells, 2.5 μm long). We took advantage of this difference to look at the influence of ϕ_A on V_A in bacterial suspensions. In Fig. 1(c) we display 6 independent experiments performed with populations having a majority of 1N cells (brown, red, and green), a mixture of 1N and 2N cells (black), a majority of 2N cells (pink, blue). For each sample, ϕ_A was taken from suspensions showing an average of 100 or 200 bacteria in the observation field [represented by (1) and (2) in Fig. 1(c), respectively]. ϕ_A shows little influence on V_A, but V_A could be different according to bacteria position within the cell cycle. In the case of the Au-Pt rods, Fig. 1(f) does not show a stronger dependence of V_A on ϕ_A. This low dependence on ϕ_A is due to the low swimmer concentration of the suspension, where no collective behavior is observed.

In the following, we will relate the motion of the passive tracers to the number of active swimmers and their mean velocity. Passive tracer trajectories were analyzed (about 10 tracks in a 300-image video at 1 frames/s for bacteria and 40 s sequences at 8 frames/s for Au-Pt rods). No significant stickiness between the spheres and the swimmers was observed, and those rare cases were eliminated. From these tracks, the mean passive tracer diffusion coefficient D_P was extracted consistently using two independent methods. The first one applied mean square displacements at long times (diffusive regime [1]) of individual particles; the second one used particles as pairs in order to eliminate residual drift. In Fig. 2 the passive tracer diffusivities are displayed for all the experiments presented in Figs. 1(c) and 1(f). D_P values are displayed as a function of $J_A = n_A V_A$, which we call the "activity flux." For experiments performed with the same tracer size, we observe a collapse of all data onto a linear curve:

$$D_P = D_P^B + \beta J_A, \tag{1}$$

where D_P^B is the Brownian diffusivity of the latex particles in the vicinity of the surface, in the absence of swimmers. Note that, due to lubrication forces, this value is smaller than the Brownian diffusivity expected in the bulk ($D_B = k_B T/3\pi\eta d$) and, for the parallel motion, they are related by $D_P^B = \alpha D_B$, where $\alpha < 1$ is the parallel drag correction factor [24–26]. The α factor depends on the bead distance to the surface, vanishing at contact and going asymptotically to one at large distances. The beads are not at a fixed distance to the surface, but they are distributed according to Boltzmann's factor $\exp(-m^* gz/k_B T)$, where m^* is the

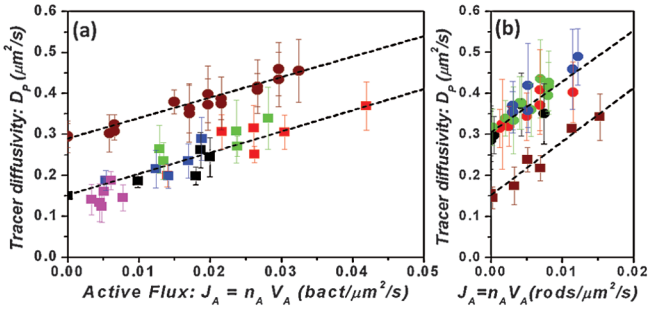

FIG. 2 (color). Enhanced diffusivity D_P of passive tracers as a function of J_A. Squares and circles represent tracer of 2 and 1 μm diameters, respectively. Panel (a) corresponds to the bacterial suspensions. Each color represents an experiment performed over a range of bacterial dilution. Panel (b) corresponds to suspensions of Au-Pt rods: green, blue, and black circles correspond to various H_2O_2 concentrations (from 2.5% to 20%). The dashed lines are linear fits and the error bars are standard deviations (the rest of the colors defined in Fig. 1 and text).

buoyant mass. Therefore, α must be averaged with this factor. In the active rods experiments we obtained $\alpha = 0.7$ both for the buoyant $d = 1\ \mu$m and $d = 2\ \mu$m latex spheres, values that agree with the theoretical prediction given above ($\alpha = 0.64$ for $d = 1\ \mu$m and $\alpha = 0.74$ for $d = 2\ \mu$m). In the experiments with bacteria, the suspended beads are almost isodense, but they sediment anyway. The experimental fit gives $\alpha = 0.85$. This value allows us to infer the density mismatch $\Delta\rho = 0.008$ g/ml, which is consistent with the experimental preparation. The collapse holds also for bacterial populations at different maturation stages (1N, 2N, or unsynchronized mixtures). From dimensional analysis of expression (1), it can be seen that the prefactor β is a length to the fourth power. It varies from 5 $\mu m^4 = (1.5\ \mu m)^4$ for bacteria to 13 $\mu m^4 = (1.9\ \mu m)^4$ for active rods, but seems to be almost independent of the passive tracer size. Close to the plates the hydrodynamic perturbations created by the swimmers decay as the inverse cube of the distance, faster than in the bulk [27]. Therefore, at low concentrations, the enhanced diffusivity in (1), proportional to n_A and V_A, can be understood as a result of a series of elementary encounters between active swimmers and the tracers: the number of encounters per unit time is proportional to $n_A V_A$. On the other hand, low Reynolds dynamics points out that the tracer displacement at each encounter is independent of the swimmer velocity and depends only on geometrical factors: the impact parameter, the swimmer dimensions, and weakly on the tracer size through the Faxén correction of passive transport [28,29]. The β factor comes out from averaging the tracer's displacements, but its computation is difficult because it requires a correct modeling of the near field interactions between the swimmer and the tracer, taking into account the detailed swimmer geometry and the effect of the surface.

In conclusion, we have characterized active momentum transfer close to solid surface for two active suspensions (wild-type bacteria and artificial self-propelled swimmers). The effect was measured using the diffusion enhancement of a passive tracer. In spite of the *a priori* complexity of the hydrodynamics and essential differences in the propulsion modes, we demonstrated that the effect emerges quantitatively in a similar way. The resulting diffusion coefficient is the sum of the Brownian contribution near the wall and an active part, proportional to the product of the density of active swimmers and their mean velocity at the surface. The proportionality factor, scaling as the 4th power of a micron size length, encompasses the details of momentum transfer for each swimmer and is found to be weakly (if at all) sensitive to the probe diameter. Importantly, discriminating between so-called ''active'' and ''random'' swimmers was crucial for predicting the induced transport phenomenon, and we have developed a protocol to make such a distinction. The functional dependence of the enhanced diffusivity is explained in terms of successive interactions between a single swimmer and the tracer, each one producing a net displacement. Our results justify the pursuit of a quantitative determination of such encounters based on simple hydrodynamic models [28].

We thank D. Grier for discussions on the tracking programs, financial support from PGDG Foundation, the Alfa-SCAT program, Sesame Ile-de-France, Fondecyt Grants No. 1061112, No. 1100100, Anillo Grant No. ACT127, No. ECOS C07E08, and NSF No. 0820404.

[1] X.-L. Wu and A. Libchaber, Phys. Rev. Lett. **84**, 3017 (2000).
[2] D. T. N. Chen *et al.*, Phys. Rev. Lett. **99**, 148302 (2007).
[3] D. Saintillan and M. J. Shelley, Phys. Rev. Lett. **99**, 058102 (2007); Phys. Rev. Lett. **100**, 178103 (2008).
[4] Y. Hatwalne *et al.*, Phys. Rev. Lett. **92**, 118101 (2004).
[5] C. Dombrowski *et al.*, Phys. Rev. Lett. **93**, 098103 (2004).
[6] K. C. Leptos *et al.*, Phys. Rev. Lett. **103**, 198103 (2009).
[7] S. Rafaï, L. Jibuti, and P. Peyla, Phys. Rev. Lett. **104**, 098102 (2010).
[8] W. F. Paxton *et al.*, J. Am. Chem. Soc. **126**, 13 424 (2004).
[9] R. A. Simha and S. Ramaswamy, Phys. Rev. Lett. **89**, 058101 (2002).
[10] A. Sokolov and I. S. Aranson, Phys. Rev. Lett. **103**, 148101 (2009); B. Haines *et al.*, Phys. Rev. E **80**, 041922 (2009).
[11] N. Darnton *et al.*, Biophys. J. **86**, 1863 (2004).
[12] A. Sokolov *et al.*, Proc. Natl. Acad. Sci. U.S.A. **107**, 969 (2009), andreferences therein.
[13] G. Gregoire, H. Chate, and Y. Tu, Phys. Rev. E **64**, 011902 (2001).
[14] M. Ibele, T. E. Mallouk, and A. Sen, Angew. Chem., Int. Ed. **48**, 3308 (2009).
[15] A. P. Berke *et al.*, Phys. Rev. Lett. **101**, 038102 (2008).
[16] E. Lauga *et al.*, Biophys. J. **90**, 400 (2006).
[17] P. D. Frymier *et al.*, Proc. Natl. Acad. Sci. U.S.A. **92**, 6195 (1995).
[18] G. Li, L.-K. Tam, and J. X. Tang, Proc. Natl. Acad. Sci. U.S.A. **105**, 18 355 (2008).
[19] M. A. S. Vigeant and R. M. Ford, Appl. Environ. Microbiol. **63**, 3474 (1997).
[20] B. M. Prüß and P. Matsumura, J. Bacteriol. **179**, 5602 (1997).
[21] R. Allman, T. Schjerven, and E. Boye, J. Bacteriol. **173**, 7970 (1991).
[22] Y. Wang *et al.*, Langmuir **22**, 10 451 (2006).
[23] J. L. Moran, P. M. Wheat, and J. D. Posner, Phys. Rev. E **81**, 065302 (2010).
[24] H. Brenner, Chem. Eng. Sci. **16**, 242 (1961); A. J. Goldman, R. G. Cox, and H. Brenner, Chem. Eng. Sci. **22**, 637 (1967).
[25] P. Holmqvist, J. K. G. Dhont, and P. R. Lang, Phys. Rev. E **74**, 021402 (2006).
[26] P. Huang and K. S. Breuer, Phys. Rev. E **76**, 046307 (2007).
[27] J. R. Blake and A. T. Chwang, J. Eng. Math. **8**, 23 (1974).
[28] J. Dunstan, M.Sc. thesis, Universidad de Chile, 2010; J. Dunstan *et al.* (to be published).
[29] J. Happel and H. Brenner, *Low Reynolds Number Hydrodynamics: With Special Applications to Particulate Media* (Kluwer, The Hague, 1983).